Decoding metrics for slow frequency-hopped DPSK systems

Yu T. Su

Indexing terms: Radiocommunication, Frequency hopping, Spread spectrum, Noise jamming, Phase shift keying

Abstract: A variety of soft-decision decoding metrics for slow frequency-hopped, differential phase shift keyed spread-spectrum systems are studied. The computational cut-off rates in the presence of partial band noise jamming for these metrics are analysed. The usefulness of various degrees of side information, the effectiveness of limiting and quantisation when side information is not available, and the importance of a judicious choice of the quantisation step size are demonstrated. Monte-Carlo type simulations for the system encoded by Odenwalder's (7, 1/2) code are conducted, the resulting BERs reveal that close approximations can be attained by estimations calculated from a known closed-form formula.

1 Introduction

Because of their simplicity and robustness, frequency-hopped (FH) differential phase shift keyed (DPSK) spread-spectrum systems have been proposed by many authors [1–8] to combat intentional interferences. An FH system is called fast FH if its hopping rate is greater than one hop per channel symbol, otherwise it is called a slow FH system. Because of the difficulty of maintaining the phase coherency among different hops, fast FH/DPSK systems remain only a theoretical interest, at least for the time being.

Antijam (AJ) capabilities for 2- and 4-ary slow FH/DPSK systems were analysed by Houston [1]. Cooper and Nettleton [2] proposed a Hadamard-coded fast FH/DPSK system to provide a mobile radio service; both linear and nonlinear receivers had been considered [2, 3]. Hard-decision decoded FH/DPSK performance in partial band noise jamming (PBNJ) can be found in Reference 4. Lee and Miller [5] derived the uncoded bit error rate (BER) for a fast FH/DPSK system, also in PBNJ. Simon [6] generalised Houston's analysis to M-ary FH/DPSK in partial band multitone jamming (PBMTJ) and in PBNJ [7]. Taking the entropy of an FH carrier as a design parameter to be optimised, Lindsey *et al.* [8] recently obtained new results on M-ary slow FH/DPSK in PBMTJ. Each of these investigations has considered only either the uncoded or hard-decision decoded system behaviours, and many of them have assumed zero thermal noise in their analysis. Simulation results for soft-decision performance of coded FH/DPSK in the presence of PBNJ or Rayleigh fading was recently reported by Yost [17]. However, Yost concentrated his efforts on comparison of various demodulator structures rather than metric design, and did not give any analytical results. It is the purpose of this paper to analyse the effects of side information and a variety of soft-decision decoding metrics on the performance of a slow FH/DPSK receiver in the presence of PBNJ, taking thermal noise into consideration. The following Section provides a description of the FH/DPSK system and defines the basic system parameters. A variety of decoding metrics and their cut-off rates are examined in subsequent Sections. The decoding metrics are divided into two categories according to their operation scenarios; those with perfect side information and those with no or imperfect side information. As an application example, the BER performance of a (7, 1/2) convolutional-encoded system is evaluated and it is demonstrated therein that the analysis yields a very close approximation to the simulation results.

2 System description and assumptions

The slow FH/DPSK receiver to be considered here is depicted in Fig. 1. Other implementations of DPSK demodulation that yield the same statistics are possible [17]. The received waveform is dehopped and then mixed in both I and Q channels. The down-converted signals are filtered by the integrate-and-dump detectors and delayed by a chip time T_c (which is equal to a code symbol time T_s because of the slow hop assumption). In both I and Q channels, the sum and difference of two adjacent bits separated by the chip time are squared and the corresponding terms are added. The difference of these two outputs is then passed through an N $(=2^k)$ level quantiser. Unless the code used in the system has burst error correcting capability, a deinterleaver must be inserted between the quantiser output and the decoder input to put the interleaved coded data back in order and at the same time to randomise possible burst demodulation errors. In the subsequent analysis, perfect interleaving/deinterleaving will be assumed so that the 'channel' between the encoder output and the decoder input becomes memoryless. Moreover, although a finite-bit quantisation is always necessary in practice, it will be assumed that infinite-bit precision is possible so that the following two cases are to be separately discussed: $N = \infty$ (no quantisation) and $N < \infty$ (finite-bit quantisation.

BER or cut-off rate performance is usually measured with respect to the required E_b/N_0, where N_0 = one-sided thermal noise power spectral density, $E_b = S/R_b$,

Paper 8902I (E8), first received 7th March 1991 and in revised form 1st April 1992

The author is with the Microelectronic and Information Systems Research Center and the Department of Communication Engineering, National Chiao Tung University, Hsinchu, Taiwan

S = received signal power, and R_b = information bit rate. The PBNJ jamming effect is maximised if its total available power J can be concentrated on a band of μW Hz, where $0 < \mu \leqslant 1$ is called the fraction of the band jammed and W is the total hopping bandwidth. Therefore, if a communication link is hit by a PBNJ (which occurs with probability μ) and if a random hopping pattern is assumed, then the signal is corrupted by an equivalent thermal noise with power spectrum level equals to $N_{J'} \triangleq N_0 + N_J/\mu$, $N_J \triangleq J/W$. Owing to the slow-hopping nature of the system, it is reasonable to assume that channel synbols in the same hop are either all jammed or all unjammed, hence two consecutive symbols used in demodulating a coded symbol are corrupted by a noisy component with the same statistic. For a system employing a rate R_s code, one has $R_s E_b/N_J = E_s/N_J$ where $E_s = S/R_s$ = energy per symbol. Hence if one has the required E_s/N_J to achieve a cut-off rate R_0, one can easily find out the required $E_b N_J$ via the above relation if the code used has a rate less than or equal to R_0.

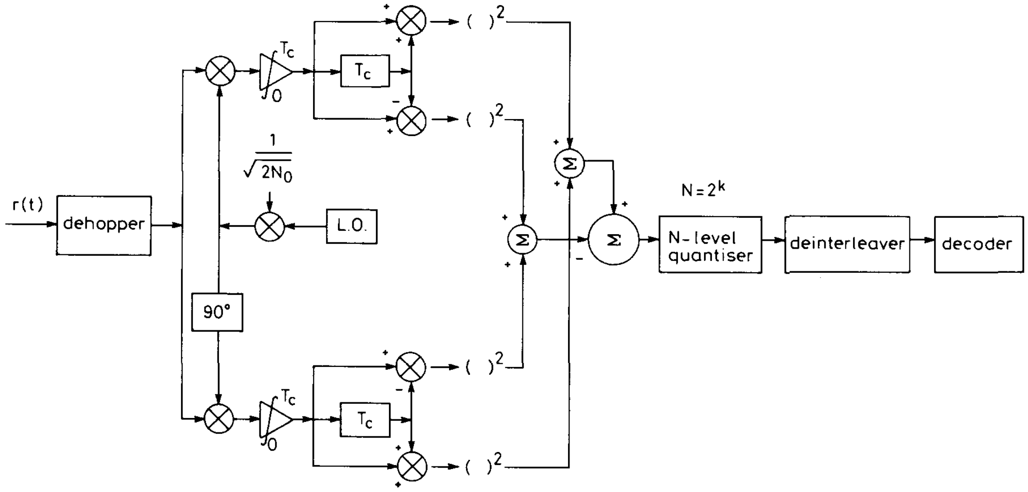

Fig. 1 *Block diagram of soft-decision decoded FH/DPSK receiver*

3 Metrics with perfect side information

A decoding metric is used to measure the distance between the demodulated waveform and the desired code symbol. The effect of a decoding metric on the decoded bit error rate (BER) is expressed by the following equations [9, 11], which relate the BER and the computational cut-off rate R_0 to the decoding metric

$$BER \leqslant G(D) \tag{1a}$$

$$R_0 = 1 - \log_2(1 + D) \tag{1b}$$

where R_0 can be regarded [9] as the practically achievable reliable data rate per coded symbol and the functional form $G(\cdot)$ is to be determined by the specific code used. The parameter D for a memoryless channel is defined by [9, 11]

$$D = \min_{\lambda \geqslant 0} D(\lambda) = \min_{\lambda \geqslant 0} E\{\exp[\lambda(m(y, x'; z) - m(y, x; z))] \mid x\}_{x' \neq x} \tag{2}$$

where y is the decoder input, x' and x are different encoder outputs (which in the case of binary channels may be represented by 1 or -1), and z stands for side information such as knowledge of a jammer's presence, the associated jamming power etc. [9]. The optimal decoding metric in the sense of minimising BER is the so-called maximum-likelihood (ML) metric, $m(x, y; z) = \log[p(y \mid x, z)]$, $p(y \mid x, z)$ being the conditional PDF of the demodulator output y given that the code symbol x has been transmitted and side information z is provided. When side information is not available, the ML metric then becomes $m(x, y; z) = m(x, y) = \log[p(y \mid x)]$. Note that the cut-off rate defined in eqn. 1a is a generalisation of the one associated with the so-called channel reliability function [13] in the sense that the latter is valid for ML metrics only whereas the former can be defined for arbitrary metrics [9].

Under the perturbation of the additive white Gaussian noise (AWGN), the binary DPSK demodulator output behaves as the difference of a squared Rician random variable Z_s and a squared Rayleigh random variable Z_d. The probability density function (PDF) of such a random variable can be derived from convoluting the PDFs of Z_s and $-Z_d$ or from taking inverse transform of the characteristic function of $Z_s - Z_d$ [14, 16]

$$p(y; x) = 0.5e^{y - x/2}Q[\sqrt{(x)}, 2\sqrt{(y)}], \quad y > 0$$
$$= 0.5e^{y - x/2} \quad y < 0 \tag{3a}$$

where

$$Q(a, b) = \int_b^\infty v \exp[-(a^2 + v^2)/2] I_0(av)\, dv \tag{3b}$$

$I_0(\cdot)$ is the modified Bessel function of the first kind of order zero, and $x = 2E_s/N_0$ or $2E_s/N_{J'}$, depending on whether a PBNJ is present. It can be shown [7] that, for ML decoding with perfect side information,

$$D = \int_y \sqrt{\{p(y \mid -1)p(y \mid 1)\}}\, dy$$

where $p(y \mid i)$ is the probability density function (PDF) of the demodulator output given that the code symbol i ($i = -1$ or 1), has been transmitted. Substituting eqn. 3a

into the above equation, one obtains

$$D = (1 - \mu)\exp(-\beta_0)\int_0^\infty \sqrt{\{Q(2\beta_0, 2\sqrt{y})\}}\,dy + \mu\exp(-\beta_J)\int_0^\infty \sqrt{\{Q(\sqrt{2\beta_J}, 2\sqrt{y})\}}\,dy \quad (4)$$

where $\beta_0 = E_s/N_0$ and $\beta_J = E_s/N_{J'}$. The perfect side information assumption here implies

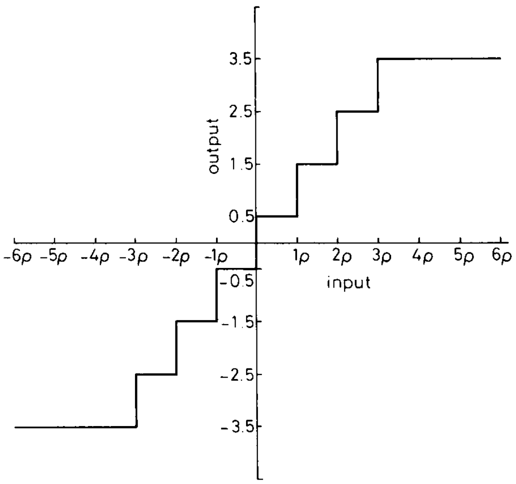

Fig. 2 *N-level quantiser: $N = 8$*

(i) the presence or absence of the jammer is always detected without error

(ii) the magnitudes of the thermal noise power spectral density N_0 and the jamming power at each hop can be perfectly estimated

(iii) the information obtained in (i) and (ii) is used to generate the corresponding ML metric during the course of decoding.

To implement an ML decoding metric $\log[p(y|x)]$, the jammer state must be made available. Moreover, an ML decoding metric which is optimal for one kind of jammer is bound to be less superior for other jammers. Since most of the time the communication link is free of jamming, the simple AWGN ML metric $m(x, y) = xy$ is usually adopted no matter whether the coding channel is AWGN or not. A mismatch will arise whenever the channel statistic deviates from the assumed one. The mismatch loss is therefore defined [11] as the difference of the required E_b/N_0 between the ML decoder and a non-ML one to achieve a given BER.

With AWGN, it has been shown [14] that the 3-bit quantisation suffers less than a 0.25 dB loss compared to the infinite-bit case. However, in the presence of jamming, as was shown in References 7 and 8, this is not the case unless side information is furnished. The reason for this is simple. When a jammed chip results in a large erroneous (i.e. incorrect sign) metric, the corresponding code word metric, which is the sum of each component (or chip) metric, will need a lot of clean chip metrics to make up for the single error. An obvious solution to this problem is to limit the maximum absolute value of the metric so that any single contaminated output from the metric convertor will not do too much damage. Hard limiting is the simplest choice. A better 'damage control' mechanism is to multiply the demodulator output y by a weighting factor C_y, which is a function of the jammer state information derived from say, an AGC circuit. For the receiver with decoding metric $m(x, y; z) = C_y xy$, where $C_y = C_J$ if y is jammed, and $C_y = C_0$ otherwise, one obtains

$$D(\lambda, \mu) = \frac{\mu}{1 - (\gamma\lambda)^2}\exp\left[\frac{\gamma\lambda\beta J}{1 + \gamma\lambda}\right] + \frac{1 - \mu}{1 - (w\lambda)^2}\exp\left[\frac{\lambda w\beta_0}{1 + w\lambda}\right] \quad (5)$$

where $w = C_0/C_J$, $0 < \lambda \leqslant \min(1/\gamma, 1/w)$, $\gamma \triangleq N_{J'}/N_0$. The inclusion of μ in the notation $D(\lambda, \mu)$ emphasises the dependence of D on μ. From eqn. 5, one can show that the optimal weighting for direct-sequence-BPSK signalling, $C_J = 1$, $C_0 = \infty$, as suggested in Reference 9, is not suitable for the FH/DPSK system in question. In fact, for $C_J = 1$,

$$\lim_{C_0 \to \infty} \min_\lambda D(\lambda, \mu) = \mu + \delta \quad (6)$$

where

$$\delta = (1 - \mu)/(1 - \eta^2)\exp[-\eta\beta_0/(1 + \eta)]$$

$$\eta = [\sqrt{\{(2 + \beta_0)^2 + 8\beta_0\}} - (2 + \beta_0)]/4.$$

If there is no thermal noise, i.e. if $\beta_0 = \infty$, then

$$D(\lambda, \mu) = \mu/(1 - \lambda^2)\exp[-\lambda\beta_J/(1 + \lambda)] \quad (7)$$

For the special case when $(C_J, C_0) = (1/N_{J'}, 1/N_0)$ one obtains

$$D(\lambda, \mu) = \mu/(1 - \lambda^2)\exp[-\lambda\beta_J/(1 + \lambda)] + (1 - \mu)/(1 - \lambda^2)\exp[-\lambda\beta_0/(1 + \lambda)] \quad (8)$$

Figs. 3 and 4 compare cut-off rates for the above three soft-decision decoders, namely the suboptimal weighting,

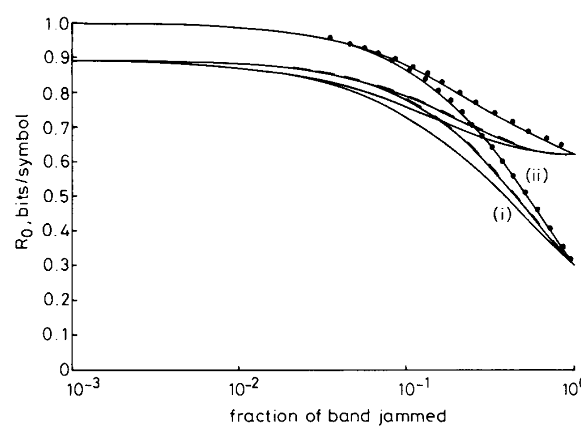

Fig. 3 *Cut-off rates for three FH/DPSK soft-decision metrics*
——— optimal weighting
– – – – optimal (finite) weighting
· · · · · · suboptical weighting
(i) $E_s/N_J = 5$ dB (ii) $E_s/N_J = 10$ dB $E_s/N_0 = 9$ dB
no quantisation

eqn. 8, the zero thermal noise case, eqn. 7, and the optimal finite weighting, eqn. 5, with w optimised. These numerical results reveal that they behave almost the same, especially in high E_s/N_0 environments. The family of weights, $\Lambda \triangleq \{(N_{J'}^{-x}, N_0^{-x}), 0.5 \leqslant x \leqslant 2\}$, was investigated via numerical search and it turns out that $x = 1$ yields the tightest Chernoff bound D. This is why eqn. 8 is chosen to represent the class Λ.

The metrics discussed so far assume an infinite bit precision in the decoding circuitry. In reality this can at best be approximated by using N-bit words, where N is large. To evaluate the decoded performance for the finite bit precision case, it is necessary to obtain the probability mass function (PMF) of the N-bit quantiser output.

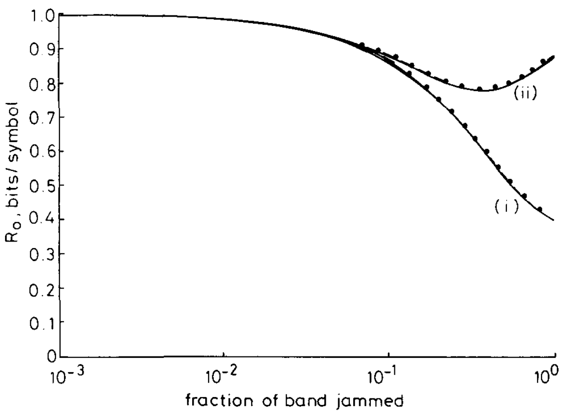

Fig. 4 *Cut-off rates for three FH/DPSK soft-decision metrics*
——— optimal weighting
- - - - optimal (finite) weighting
······· suboptimal weighting
(i) $E_s/N_J = 5$ dB (ii) $E_s/N_J = 10$ dB $E_s/N_0 = 15$ dB
no quantisation

Given the demodulator output PDF (eqn. 3), this PMF is to be derived by evaluating the difference of the corresponding probability distribution function $F(y; x)$ at the quantiser input thresholds. Using the technique of integration by parts and the definition of Marcum's Q function (eqn. 3b) one obtains [16]

$$\begin{aligned} F(y; x) &= 1 - Q[\sqrt{(2x)}, \sqrt{(2y)}] \\ &\quad + 0.5e^{y - x/2}Q[\sqrt{(x)}, 2\sqrt{(y)}] \quad y > 0 \\ &= 0.5e^{-(x/2 - y)} \quad y < 0 \end{aligned} \tag{9}$$

It follows that the PMF for the output of the N-level quantiser shown in Fig. 2 is given by

$$\begin{aligned} &\Pr(z = n + 1/2 \mid \gamma) \\ &\triangleq P_n(\gamma) \\ &= F((n + 1)\sigma) - F(n\sigma) \quad -N/2 + 1 < n < N/2 - 1 \\ &= 1 - F((N/2 - 1)\sigma) \quad n = N/2 - 1 \\ &= F((1 - N/2)\sigma) \quad n = -N/2 + 1 \end{aligned}$$

Defining $P_n(\gamma) \triangleq \Pr(z = n + 1/2 \mid \gamma)$ then, for a slow FH/DPSK receiver with the N-level quantiser (Fig. 8), one obtains

$$\begin{aligned} D(\lambda, \mu) = \sum_{n=-N/2}^{N/2-1} &[\mu P_n(N_{J'}/N_0) + (1 - \mu)P_n(1)] \\ &\times \exp[-\lambda(n + 0.5)] \end{aligned} \tag{10}$$

where

$$\begin{aligned} P_n(\gamma) &= Q[\sqrt{(2x)}, \sqrt{(2n\rho/\gamma)}] \\ &\quad - Q[\sqrt{(2x)}, \sqrt{(2(n + 1)\rho/\gamma)}] \\ &\quad - 0.5e^{-x/2}[e^{n\rho/\gamma}Q(\sqrt{(x)}, 2\sqrt{(n\rho/\gamma)}] \\ &\quad - e^{(n+1)\rho/\gamma}Q[\sqrt{(x)}, 2\sqrt{(n + 1\rho/\gamma)}] \\ &\qquad 0 \leqslant n < N/2 - 1 \end{aligned} \tag{11a}$$

$$\begin{aligned} &= Q[\sqrt{(2x)}, \sqrt{(2(N/2 - 1)\rho/\gamma)}] \\ &\quad - 0.5Q[\sqrt{(x)}, 2\sqrt{(N/2 - 1)\rho/\gamma}] \\ &\quad \times e^{(N/2-1)\rho/\gamma - x/2} \quad n = N/2 - 1 \end{aligned} \tag{11b}$$

$$\begin{aligned} &= 0.5e^{-x/2}(e^{(n-1)\rho/\gamma} - e^{n\rho/\gamma}) \\ &\qquad -N/2 + 1 < n < 0 \end{aligned} \tag{11c}$$

$$= 0.5e^{-(x/2 - N/2 + 1)} \quad n = -N/2 + 1 \tag{11d}$$

and where ρ = normalised step size.

In the above derivations it was assumed that the knowledge of the jammer's presence or absence is not available, and thus the receiver uses the same ρ all the time. However, as can be seen from the expressions for $P_n(\gamma)$, the performance is dictated by the quantiser step size ρ. It is well known that, if the input signal amplitude is not uniformly distributed, then the so-called 4σ-loading rule [12] calls for a quantisation step size $\rho = 8\rho_0/N$, where N is the number of quantisation levels and ρ_0 is the root mean square value of the input waveform. For the FH/DPSK receiver, it is easy to show that $\rho_0 = \sqrt{[2(1 + E_b/N_0)]}$ if the only noise component is AWGN. Although the 4σ-loading rule is optimal for minimal quantiser overload in AWGN, it may no longer be a proper choice when a PBNJ is present or under other design criteria. Figs. 5–7 illustrate the effect of the step size on R_0 with the assumption that the same step size was used for both jammed and unjammed situations. All the data were obtained with a 3-bit quantiser. These results are in direct contrast to the AWGN case [15], where the choice of the step size is not crucial to the BER performance. Numerical results [16] indicate that

(a) no single step size is the global optimal one

(b) the choice of ρ is less sensitive if μ is small and E_s/N_0 is high

(c) the optimal ρ corresponding to the worst μ is in proportion to E_s/N_0

(d) the optimal ρ is insensitive to $E_s/N_{J'}$.

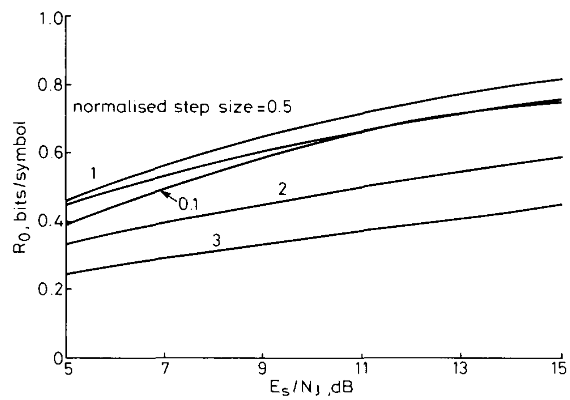

Fig. 5 *Effect of the quantiser step size ρ on cut-off rate performance*
$E_s/N_0 = 9$ dB

When the number of bits is only one ($N = 1$) the decoding metric becomes the hard-decision metric which yields the well known bound

$$D(\mu) = 2[P_e(1 - P_e)]^{1/2} \tag{12}$$

where P_e is the uncoded BER. When the jammer's state is perfectly known, one can use that information to weight optimally the demodulated bit sequence with $(C_J, C_0) = (1, \infty)$. In such a case, $D(\mu)$ should be computed with

$$P_e = \mu/2 \exp(-2\beta_0) \tag{13}$$

Fig. 8 illustrates the worst-case cut-off rate performance for four decoding metrics, all with perfect side information, namely, the hard-decision metric (eqn. 13), the sub-optimal weighting metric (eqn. 8), the 3-bit quantised metric with the step size optimised for jammed and unjammed conditions separately, and the ML metric (eqn. 4). The worst case means that the jammer chooses, from all possible μ, the one that forces the system to have the smallest cut-off rate. It is noticed that the last three metrics perform equally well at high E_s/N_J. They all essentially belong to the same category of receiver which puts different weights on contaminated and uncontaminated demodulator outputs.

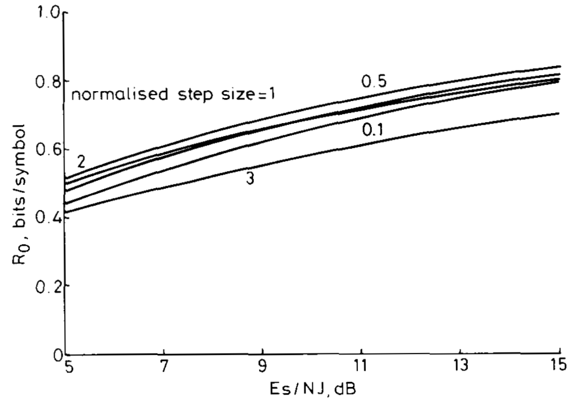

Fig. 6 *Cut-off rate as a function of E_s/N_J and quantiser step size ρ*
$E_s/N_0 = 15$ dB

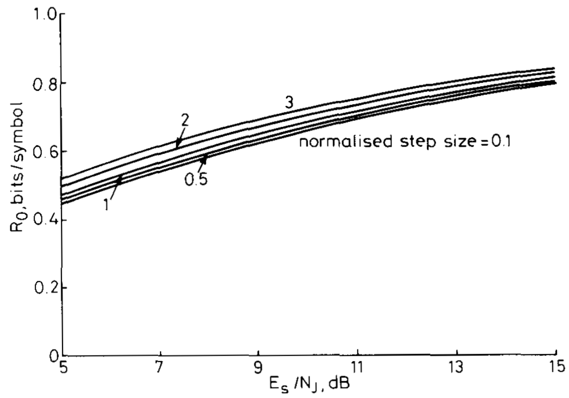

Fig. 7 *Cut-off rate as a function of E_s/N_J and quantiser step size ρ*
$E_s/N_0 = 25$ dB

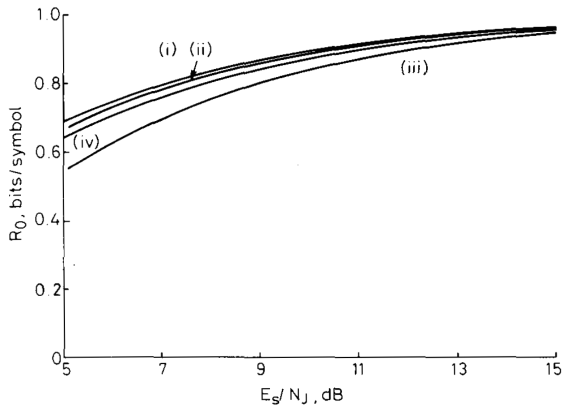

Fig. 8 *Cut-off rate performance with perfect side information*
(i) Maximum likelihood metric
(ii) Optimal weighting without quantisation
(iii) Hard decision
(iv) Optimal 3-bit quantisation

4 Metrics with no or imperfect side information

Note that all these decoding metrics require perfect side information about the jammer state. In practice, the jammer state is never perfectly known, hence the numerical results obtained can be used only as the baseline performance for each metric. This Section will examine the effect of the absence of such perfect side information.

The first case of practical interest is the soft metric (C_J, C_0) of eqn. 5. When no side information is available, no weighting is necessary or possible. Substituting $(C_J, C_0) = (1, 1)$ into eqn. 5, one obtains

$$D(\lambda, \mu) = \mu \exp[-\lambda\gamma\beta_1/(1 + \gamma\lambda)]/[1 - (\gamma\lambda)^2] + (1 - \mu) \exp[-\lambda\beta_2/(1 + \lambda)]/(1 - \lambda^2) \quad 0 \leqslant \lambda < 1 \tag{14}$$

For the hard-decision metric, the uncoded BER

$$P_e = (1 - \mu)/2 \exp(-E_b/N_0) + \mu/2 \exp(-E_b/N_{J'}) \tag{15}$$

should be used in place of eqn. 13 in evaluating $D(\mu)$ (see eqn. 12). The ML metric without the jammer state gives the following equation

$$D(\lambda, \mu) = \frac{\mu e^{-\beta_J}}{2\gamma}\left(\int_0^\infty e^{y(2\lambda - 1/\gamma)} Q^\lambda[\sqrt{(2\beta_0)}, 2\sqrt{(y)}]\, dy + \int_0^\infty e^{-y(2\lambda - 1/\gamma)} \frac{Q[\sqrt{(2\beta_J)}, 2\sqrt{(y/\gamma)}]}{Q^\lambda[\sqrt{(2\beta_J)}, 2\sqrt{(y/\gamma)}]}\, dy\right) + \frac{(1-\mu)e^{-\beta_0}}{2}\int_0^\infty \{e^{y(2\lambda - 1)} Q^\lambda[\sqrt{(2\beta_0)}, 2\sqrt{(y)}] + e^{-y(2\lambda - 1)} Q^{1-\lambda}[\sqrt{(2\beta_0)}, 2\sqrt{(y)}]\}\, dy \tag{16}$$

where it is assumed that the system is operating at the designed point β_0.

A family of soft metrics Λ was discussed in the preceding Section, where the finite weighting $(1/N_{J'}, 1/N_0)$ was shown to render a near-optimal performance. It was assumed there that the weighting factor could be obtained without error. Usually, it can be derived from a square-law envelope detector (or an AGC detector as it was sometimes called [5]) at an adjacent channel which is assumed to have the same noise statistics as the signal channel. Let the normalised weighting factors derived from the estimation circuitry be $((w_J N_0)^{-1}, (w_0 N_0)^{-1}) \triangleq (C_{J'}, C_{0'})$; then the corresponding Chernoff bound is given by

$$D(\mu; w_J, w_0) \triangleq \min_{0 \leqslant \lambda < \lambda_0} D(\mu, \lambda; w_J, w_0) \tag{17a}$$

where

$$\lambda_0 \triangleq 1/\max(\gamma/w_J, 1/w_0) \tag{17b}$$

and

$$D(\lambda, \mu; w_J, w_0) = \mu/[1 - (\lambda\gamma/w_J)^2] \times \exp[-\lambda\gamma\beta_J/(w_J + \lambda\gamma)] + (1 - \mu)/[1 - (\lambda/w_0)^2] \times \exp[-\lambda\beta_0/(w_0 + \lambda)] \tag{17c}$$

If the weighting factors are derived from an envelope detector as just mentioned, then the average Chernoff bound is

$$D(\mu) = \int_0^\infty \int_0^\infty \gamma^{-1} D(\mu; w_J, w_0) \times \exp[-(w_J/\gamma + w_0)]\, dw_J\, dw_0 \qquad (18)$$

Fig. 9 illustrates the cut-off rate performance for

(i) soft decision without side information (eqn. 14)
(ii) hard decision
(iii) ML decoding without side information (eqn. 16)
(iv) 3-bit quantisation metric without optimising step size
(v) soft decision with imperfect AGC weighting.

The case of perfect AGC weighting is also included for the convenience of comparison. In all cases, the worst μ values (denoted by μ^*) which minimise R_0 are assumed, i.e. $D(\mu^*) \triangleq \max_{0 \leqslant \mu \leqslant 1} D(\mu)$. As expected, the R_0 of the unweighted and unquantised metric (eqn. 14) is the worst one. The mismatch loss for this case is phenomenal; for example it is greater than 13 dB at $R_0 = 1/2$. But by using a hard limiter, one can easily recover more than 10 dB of the degradation. The finite-bit quantisation metric is insensitive to the variation of channel statistic as was mentioned before. The AGC weighting metric performs poorly at low E_s/N_J but gradually catch up with the ML metric at high $E_s/N_{J'}$. This is a result of the fact that the envelope detector is not a reliable noise power estimator at low $E_s/N_{J'}$. To demonstrate the utility of the cut-off rate performance, the error rate of Odenwalder's (7, 1/2) coded system is evaluated in the following Section. One can also see more clearly the relative performance improvements or degradations of each metric with respect to a fixed BER.

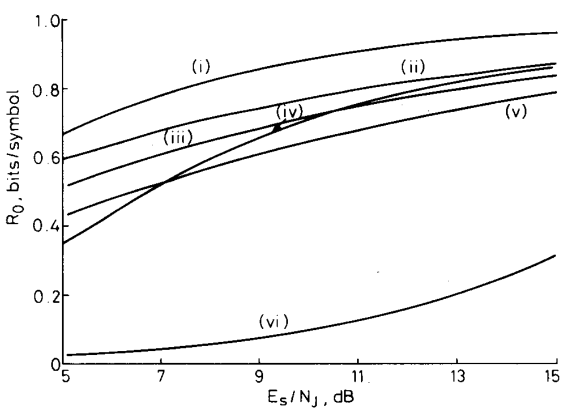

Fig. 9 *Cut-off rate performance*

(i) Soft decision with optimal weighting and perfect side information
(ii) ML metric with imperfect side information
(iii) 3-bit quantisation without side information
(iv) Soft decision with imperfect AGC weighting
(v) Hard-decision
(vi) No weighting

5 BER evaluation-comparison of two formulas

The BER performance of a convolutional encoded, three-bit soft-decision Viterbi-decoded system is presented in this Section. The Odenwalder (7, 1/2) code is chosen because of its popularity [7, 9, 10, 14]. As was mentioned in Section 3, the decoded BER is related to R_0 or D via a nonlinear function. For the (7, 1/2) code, two analytical formulas are available, namely, Odenwalder's upper bound [9],

$$\text{BER} \leqslant 0.5[36D^{10} + 211D^{12} + 1404D^{14} + 11633D^{16} + \cdots] \qquad (19)$$

D being given by eqn. 11, and Weinberg's empirical formula, which relates the BER to R_0[10]

$$\log_{10}(\text{BER}) = K_1 + K_2 \log_{10}\left\{\frac{2^{1-R_0} - 1}{1 + \exp[a(R_0 - b)]}\right\} \qquad (20)$$

where $K_1 = \log_{10}(102.31)$, $K_2 = 11.668$, $a = 3.017$ and $b = 1.602$. The thicker curves in Figs. 10 and 11 were

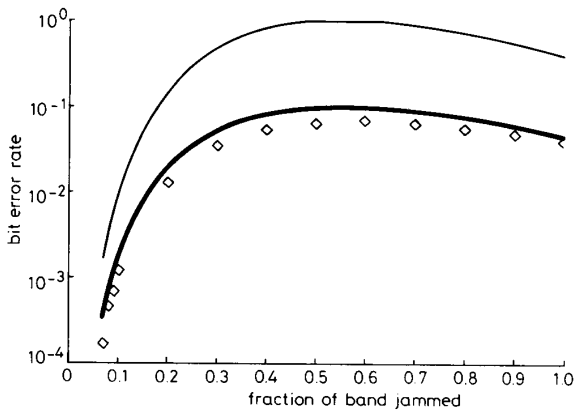

Fig. 10 *BER estimation*

—— Weinberg's formula
—— Odenwalder's upper bound
◇ Simulation
$E_b/N_0 = 9$ dB; $E_b/N_J = 7.5$ dB

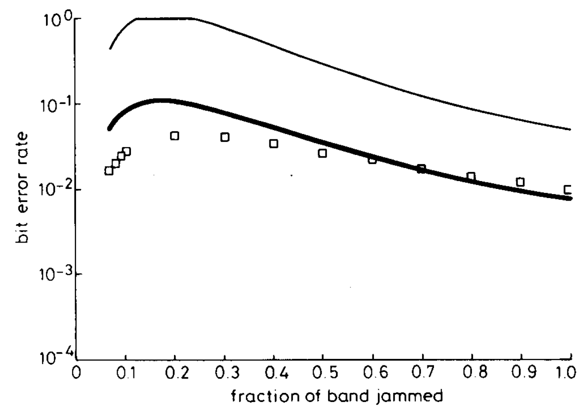

Fig. 11 *BER estimation*

—— Weinberg's formula
—— Odenwalder's upper bound
□ Simulation
$E_b/N_0 = 15$ dB; $E_b/N_J = 5$ dB

computed from the former, and the thinner curves were computed from the latter. The constants in eqn. 20 were derived from established simulation data for the Gaussian channel with 3 bit quantisation. It is found that the behaviour of the decoded BER as a function of μ is consistent with earlier reports [1–8] and eqns. 19 and 20 both predict a similar trend and the same worst case μ. Also shown in these two figures are some Monte-Carlo simulation results which tell us that Weinberg's formula (eqn. 15) is uniformly tighter than Odenwalder's upper bound (eqn. 14) by an order of magnitude. The slight discrepancies between the simulation and formula-derived results are due to the fact that Weinberg's formula assumed a quantised ML metric. Fig. 12 is the BER performance of the (7, 1/2) coded system for various metrics, converted from parts of Figs. 8 and 9, i.e. eqn. 20 is used to obtain BER from R_0. For the convenience of comparison, the BER curves are plotted against E_s/N_0, the corresponding E_b/N_0 being 3 dB higher. Conclusions similar to those in the preceding Section can be made.

It is revealed that, when the BER is 10^{-5}, the optimal weighting metric is only 0.3 dB away from the best performance if perfect side information is supplied. The replacement of perfect side information with AGC estimation does not cause too much degradation (e.g. a 1.1 dB loss even for an estimation as bad as (1.5, 0.1)). One also observes that the mismatch loss for the ML metric without side information is about 2 dB. The case of 3-bit quantisation without the knowledge of the jammer state suffers another 1.8 dB loss whereas the hard-decision metric has a mismatch loss of 6 dB. In other words, the increase of quantisation resolution from 1 bit to 3 bits can easily give 4.2 dB improvement. The metric of soft decision without weighting is not presented in Fig. 12 because the corresponding BER is higher than

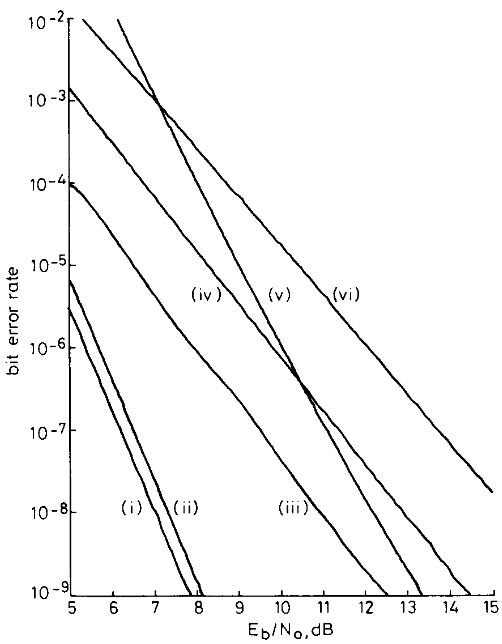

Fig. 12 *BER performance*

(i) ML metric with perfect side information
(ii) Soft-decision with optimal weighting and perfect side information
(iii) ML metric without side information
(iv) 3-bit quantisation without side information
(v) Soft decision with imperfect AGC weighting
(vi) Hard decision without side information

10^{-2} within the range of interest. However, computations can show that, at a 10^{-5} error rate, the simple hard-decision metric recovers more than the 10 dB loss suffered by the soft-decision/no-side-information metric.

6 Conclusion

An analytic approach to evaluate the coded performance of practical FH/DPSK receivers in the presence of partial band noise jamming has been presented. A variety of decoding metrics have been considered and compared. The effectiveness of quantisation is most convincing when side information is not available; an improvement of more than 10 dB is obtained by resorting to the simple hard limiter. The Viterbi-decoded performance of the Odenwalder (7, 1/2) convolutional code is evaluated with two formulas. Comparison with simulation data has revealed that Weinberg's empirical formula is an excellent approximation for BER performance estimations in PBNJ. This result indicates that the BER performance of the 3-bit soft-decision metric is about 2 dB away from that of the corresponding ML metric, and that the AGC weighting scheme is recommended if an operating E_b/N_0 greater than 10.5 dB is available or if a BER less than 3×10^{-7} is required.

Besides intentional jamming, electromagnetic waveforms generated by nonhostile sources sometimes can also degrade the signal channel performance, especially when the latter link has a low power margin. As far as a FH system receiver is concerned, many broadband radio-frequency interference (RFI) waveforms, such as those resulting from noncoherent radar pulsed trains, can be treated as PBNJ as well. A practical application example is to evaluate the ship communication terminal AJ capability when the RFI comes from onboard radar signals. Moreover, it was recently shown [8] that PBNJ is as effective as PBMTJ against FH/DPSK systems. Thus the analysis and the numerical results presented here can be used in system designs and performance predictions, even when the assumed operating scenario is not strictly PBNJ.

7 Acknowledgment

This paper has been presented in part at the ICC '89 conference at Boston, USA, in June 1989.

8 References

1 HOUSTON, S.W.: 'Modulation techniques for communication. Part I: Tone and noise jamming performance of spread spectrum *M*-ary FSK and 2, 4-ary DPSK waveforms'. Presented at IEEE 1975 NAE Conference, June 1975
2 COOPER, G.R., and NETTLETON, R.W.: 'A spread spectrum technique for high-capacity mobile communications', *IEEE Trans.*, 1978, **VT-27**, pp. 264–275
3 MATSUMOTO, M., and COOPER, G.R.: 'Performance of a nonlinear FH-DPSK spread-spectrum receiver with multiple narrow-band interfering signals', *IEEE Trans.*, 1982, **COM-30**, pp. 937–942
4 SU, Y.T.: 'Anti-jam performance of a FH/DPSK system (I)', LinCom Corporation, TM-8520-25, 1987
5 LEE, J.S., and MILLER, L.E.: 'Error probability analysis of differential phase-shift-keyed/frequency-hopping spread-spectrum communications in the partial-band jamming environments', *IEEE Trans.*, 1982, **COM-30**, pp. 943–952
6 SIMON, M.K.: 'The performance of *M*-ary FH/DPSK in the presence of partial band multitone jamming', *IEEE Trans.*, 1982, **COM-30**, pp. 963–958
7 SIMON, M.K., OMURA, J.K., SCHOLTZ, R.A., and LEVITT, B.K.: 'Spread spectrum communications, Vol. II' (Computer Science Press, Rockville, MD, 1985)
8 LINDSEY, W.C., AN, S.H., and VACEK, R.M.: 'Performance of *M*-ary FH-DPSK systems in the presentce of jamming'. Proceedings of MILCOM'88, October 1988, pp. 34.2.1–34.2.5
9 OMURA, J.K., and LEVITT, B.K.: 'Coded error probability evaluation for antijam communication systems', *IEEE Trans.*, 1982, **COM-30**, pp. 896–903
10 WEINBERG, A.: 'The impact of pulsed RFI on the coded BER performance of the nonlinear satellite communication channel', *IEEE Trans.*, 1981, **COM-29**, -pp. 605–620
11 SIMON, M.K.: 'The impact of mismatch on the performance of coded narrow-band FM with limiter/discriminator detection', *IEEE Trans.*, 1983, **COM-31**, pp. 28–36
12 SPILKER, J.J. Jr.: 'Digital communications by satellite' (Prentice-Hall, Englewood Cliffs, NJ, 1977)
13 BLAHUT, R.E.: 'Principles and practice of information theory' (Addison Wesley, Reading, MA, 1987), pp. 183–186
14 BELLO, P.A., and NELIN, B.P.: 'The influence of fading spectrum on the binary error probabilities of incoherent and differentially

coherent matched filter receivers', *IRE Trans.*, 1962, **CS-10**, pp. 160–168
15 HELLER, J.A., and JACOBS, I.M.: 'Viterbi decoding for satellite and space communications', *IEEE Trans.*, 1977, **COM-19**, pp. 835–848
16 MARCUM, J.I., and SWERLING, P.: 'Studies of the target detection by pulsed radar', *IRE Trans.*, 1960, **IT-6**, pp. 197–202
17 YOST, R.A.: 'On the symbiotic nature of key antijamming and anti-scintillation functions for MFSK and DPSK channels', *IEEE J. Select. Areas in Commun.*, 1990, **8**, pp. 887–894